2005 American Control Conference
June 8-10, 2005. Portland, OR, USA

Optimization of Hybrid Satellite and Constellation Design for GEO-Belt Space Situational Awareness Using Genetic Algorithms

Eugene Fahnestock[1], Richard Scott Erwin[2]

Abstract— **Meeting the goals of space situational awareness requires the capabilities of imaging objects in space in the visible light band at high resolutions and tracking their positions and orbits. This paper summarizes the determination of designs for a hybrid constellation consisting of two types of satellites to provide these capabilities in the vicinity of equatorial GEO. This is cast as an optimization problem to minimize the sum of the actual cost of the system and additional performance-dependent cost components. This minimization is done over a space of parameters such as the optical subsystem aperture and semi-major axis for each satellite type. A brute-force enumeration, or gridding, of the parameter space and three slightly different varieties of genetic algorithm are used to identify solution architectures. These designs are described in numbers and illustrated. Comparisons of the performance of all solution methods in arriving at these designs are also made.**

I. INTRODUCTION

Space Situational Awareness (SSA) is of current interest to a variety of organizations. It is desired for the LEO, MEO, and GEO regions of near-earth space, but the focus for this paper is on the toroid-shaped region surrounding equatorial GEO. The reason for this choice of "target space" is the large number of satellites within it that are fulfilling mission critical roles for the United States and for which protection is desired. In this paper, the neutral term "target" refers to any object, man-made or not, active or inactive, within the above target space. Any given target may be friendly, neutral, or hostile. The first SSA goal addressed here is to identify targets and to classify them into the friendly, neutral, or hostile categories, and to do so on a continually updating basis since that target status can change at any time for various reasons. The second SSA goal addressed is prediction of any interruption or interference in the operation of any friendly target due to the presence or actions of any other target (friendly or hostile).

Two capabilities are desired to meet these goals: 1) regular and recurring high-resolution imaging of targets in the visible wavelengths so as to determine their function, if not already known as in the case of most friendly targets, and 2) continuous tracking of target position with lower resolution, or merely with sufficient radiometric signature for position identification, so that the orbits of the targets can be determined and monitored for any significant changes that might warrant a change in target classification.

[1]Student, Department of Aerospace Engineering, The University of Michigan, Ann Arbor, MI 48109, efahnest@umich.edu

[2]Air Force Research Laboratory, Space Vehicles Directorate, 3550 Aberdeen Avenue, SE, Kirtland AFB, NM 87117

It is assumed that two kinds of satellites will be needed to provide the capabilities above, leading to design of a hybrid constellation. This will consist of "observation satellites" (OBSATs) to provide the first capability and "tracking satellites" (TRACSATs) to provide the second. Few specifications or details of the physical design and orbit of each OBSAT and TRACSAT exist, due to the novelty of the problem. With this lack of requirements, a completely open trade-off exists between better system performance, in terms of providing the capabilities desired, and actual system cost. This trade-off is converted to an optimization problem, by creating cost components dependent on certain performance metrics that are summed with the "actual cost" (in dollars) to form a "total cost" (also in dollars) that is minimized.

Multiple approaches are available for solving the optimization problem, but in this case the total cost is discontinuous over the parameter space and rather complex in its computation, such that non-gradient-based methods of optimization are needed. In addition to a brute-force gridding method, a few different varieties of genetic algorithm (GA) are used herein. We shall first better formulate the optimization problem before describing the solution methods employed against it. Then we shall present results not only indicate solutions but allow for some comparison of how the solution methods perform relative to one another.

II. PROBLEM FORMULATION

A. Choice of Physical Quantities and Parameters

Many physical quantities describe the design of the hybrid satellite constellation, but only some are considered parameters varied in the optimization. These parameters are chosen for their large impact on the modeled total cost and for their not having an obvious preferred value at the start. The other physical quantities are considered fixed values or made functions of the parameters and fixed values. Table I shows all parameters (each of which exists for the two types of satellites separately) and just some of the fixed values as well. Note that the minimum feature size to be resolved on targets by OBSATs is set at 0.1 m to match with resolutions currently achievable for closer objects in LEO with current U.S. space surveillance systems [1]. Space debris populations are also often estimated as the number of objects larger than this size [2]. Also note that the number of targets is assumed at about 900 to match with a 2010 time frame, based on data gathered from various sources. The targets are randomly distributed in initial angular position in the equatorial plane, measured in an ECI frame.

0-7803-9098-9/05/$25.00 ©2005 AACC

TABLE I

PARAMETERS VARIED IN OPTIMIZATION AND SOME FIXED PHYSICAL QUANTITIES.

Parameters for Optimization
optical system aperture, diameter of primary mirror (m)**
number of satellites
semi-major axis (m)**
eccentricity**
spacing in longitude of periapsis between satellites (rad)
spacing in mean anomaly between satellites (rad)

Fixed Quantity	Value
primary reference wavelength for optics (nm)	500
minimum feature size to be resolved on targets (m)	0.1
number of targets within GEO	900
mean dimension of target for radiometry (m)	2
absorptivity of target for radiometry	0.9
emmissivity of target for radiometry	0.03
power reflection efficiency of mirror surfaces	93%
CCD quantum efficiency curve wavelength band (nm)	400–800
CCD mean quantum efficiency in band of interest	80%
CCD pixel size (microns)	24
CCD pixel grid size (# pixels on a side)	2048
CCD read noise (electrons)	5–10
CCD dark current noise (electrons/pixel/sec)	1.0
CCD minimum signal-to-noise ratio required	10
time for worst-case slewing maneuver (sec)	30
Isp for any transfer stage or kick motor, matching use of $H_2 + O_2$ chemical propulsion (sec)	430

(**Assumed uniform within each satellite type.)

B. Modeling of the Cost of Constellation / Spacecraft Designs

A highly modular approach is taken in the development of MATLAB scripts to calculate the total cost corresponding to each parameter combination. A primary code calls on a series of stand-alone functions for each major cost component of the system, and these functions can be quickly and easily interchanged or increased in number for greater modeling fidelity. Below are descriptions of the basic set of functions used in getting the results presented later.

The cost due to less-than optimal performance for OBSATs can be based on either the angular portion of GEO left uncovered by the satellites, integrated over time, or the maximum of the revisit time separating successive imaging opportunities. The former approach is simpler. For this the maximum distance out to which an object can be imaged to the desired resolution of 0.1 m (i.e. "viewing distance")is determined. The radial positions of each of the OBSATs at an instant in time is used with the radius of GEO and the viewing distance to find the angular swath of GEO within view of each OBSAT at that instant. The angles forming the forward and rear limits of each swath are examined for overlap, and the total angle of GEO within view is summed over all OBSATs after eliminating any overlap. This is done for every time step spanning the discretized period of an OBSAT, T, the time until position w.r.t. GEO is repeated. The total angle covered at each step is multiplied by Δt and summed. One minus the ratio of the resulting number to its maximum possible value of $2\pi T$ is multiplied by a penalty coefficient sized to reflect the amount of weight the designer wishes to place on the performance relative to actual cost.

For the revisit times approach, it is necessary to do a more involved calculation at each time step. The targets are randomly distributed in angular position, and both the angular velocity of each OBSAT and the distance between each OBSAT and GEO generally changes with time. The angular swaths of GEO within view at a time step are found first. Then for each one of the $N = 900$ targets, between 0 and $2M$ logical comparisons of the target's angular position with the boundaries of those swaths are made. Here M is the number of OBSATs and the number of comparisons depends on how many access swaths there are and their overlap. This determines if each target is in view or not at that instant, after which this "observation status" is compared with the stored past observation status for each target to find the largest time interval over which there is no access. All of this must be done at every time step, and the total number of time steps must be sufficient to span a period long enough to have a near repetition of all of the relative positions. Thus the computation time for evaluating OBSAT performance cost for a single parameter combination with a revisit time approach and no circular OBSAT orbit assumption is unacceptably long.

With that constraint to circular OBSAT orbits, a simple equation for revisit time results:

$$t_{revisit} = \frac{\frac{2\pi}{M} - 2\delta}{|\omega_{sat} - \omega_{geo}|}. \quad (1)$$

This indicates a tradeoff, in order to reduce revisit time, between being closer to GEO in radius for a wider instantaneous coverage swath (measured by the half-angle δ) and being farther in radius from GEO for larger difference in angular velocity, $|\omega_{sat} - \omega_{geo}|$. Even with 50 OBSATS evenly spaced on the same prograde orbit, the typical results of this tradeoff were revisit time on the order of 30+ hours. Alternatively, if just a single OBSAT were set in a retrograde orbit always within viewing distance of GEO, then revisit times would be always less than 12 hours, though slewing to track the targets would be severe. To be able to evaluate this cost component function in an acceptable time yet not be limited to only circular orbits, the angular coverage approach was used for this work rather than the revisit time approach.

Cost due to less than optimal performance for TRACSATs is found in exactly the same way as the performance cost of the OBSATs, but with replacement of the viewing distance with a much larger detection distance calculated from radiometry using CCD information, other optical system parameters, and a model of a typical worst case target's radiance. If the solar irradiance falling on such an assumed target with diameter d and absorptivity α at 1 AU from the sun is 1376 W/m^2, then the reflected portion of that radiance is given by

$$R_{reflect} = \frac{1376\,(1-\alpha)}{8\,\pi}. \quad (2)$$

The re-emitted portion of the target's radiance, given emittance ε, is determined from

$$R_{therm} = \frac{E\ 1376\ \alpha}{16\ \pi}. \tag{3}$$

Here the fraction, E, of total energy radiated away from the body that is in the 400 nm to 800 nm wavelength band is dependent on the temperature, $Temp$, given by

$$Temp = \sqrt{\frac{\alpha\ 1376}{5.6697 \times 10^{-8}\ \varepsilon\ 4}}. \tag{4}$$

The detection distance, given a power per pixel (ppp) computed from the SNR ratio, quantum efficiency, pixel size, pixel grid dimension, read noise, and dark current noise, is then

$$d_{detect} = \frac{d}{2\ \tan\left(\sin^{-1}\sqrt{\frac{4000\ ppp}{TE\ \pi^2\ \phi^2\left[R_{reflect}+R_{therm}\right]}}\right)}, \tag{5}$$

where TE is the power reflection efficiency of mirror surfaces in the optical path, and ϕ is the optical system's aperture or primary mirror diameter.

The cost component due directly to that aperture diameter within either satellite type is computed according to

$$C_{aper} = (0.33 \times 10^6)\ exp\,(1.7146\ \phi)\ M. \tag{6}$$

This equation was determined as the curve fit to collected data points for the cost and diameter of actual primary mirrors or mirror segments for space systems made to date. The exponential increase with diameter is due to the increasing difficulty of fabricating larger mirrors with sufficient dimensional accuracy to achieve diffraction limited, or nearly diffraction limited, imaging.

Another pair of cost component functions finds the cost for the ACS systems required to achieve slewing and pointing control for each satellite type. First, the angles away from the instantaneous anti-NADIR direction in the orbital plane that mark the portion of GEO in view by either an OBSAT or a TRACSAT at any instant in time are found. These angles have vertices at the satellite's current position. Their sum is reduced to π if originally greater than π, and taken as the largest angle the satellite must slew through, in the case of having to jump from viewing one target at one extreme of its GEO coverage to viewing another target on the opposite side of that coverage. The time required to make this slew maneuver is used to find the constant angular acceleration needed for a bang-bang reorientation. The angular acceleration is used with the moments of inertia to find maneuvering torque needed, and the angular momentum storage capacity of reaction wheels is taken as half the maneuver time multiplied by this maneuvering torque plus 20% margin. Reaction wheel cost is interpolated in the range of typical market costs based on how the momentum storage needed compares with the maximum and minimum available on the market. This cost is multiplied by four for the usual four-wheel redundant configuration. Pointing accuracy is calculated from the beam width of the imaging cone, in turn dependent on pixel grid size and angular resolution dictated by aperture diameter. Similar interpolation is then used to develop costs from market ranges for star cameras and gyros/IMUs. Typical market costs are also assumed for accelerometers, solar panel and antenna dish gimbals, and ACS computing and data storage hardware. All of this is summed with the reaction wheel cost and the result multiplied by the number of satellites of the current type.

Cost due to launch of the OBSATs and TRACSATs into their orbits is based on data compiled from various sources, such as [3–6], on both current and historical, domestic and international, launch systems. In particular, for each vehicle release conditions (inclination, eccentricity, instantaneous orbit radius, and instantaneous velocity) were tabulated in a spreadsheet along with the mass able to be delivered to those conditions, the cost per launch, and fairing sizes.

Within each call of either of the two launch cost component functions, the satellite final mass, without transfer stage, was first found using masses of ACS components from research of hardware on the market, plus an areal density times the area of the mirrors (from the aperture diameter), plus flat masses for other subsystems. For the subset of launch systems filtered from the spreadsheet as able to deliver this much mass to their release conditions, and also having a fairing diameter larger than the satellite's aperture (mirror) diameter, the ΔV needed for any transfer stage was calculated to match a standard three-burn transfer from the release conditions into the final satellite orbit.

From the Isp and total transfer stage ΔV, the mass of that stage is found and added to the previous total spacecraft mass. For the subset of launch systems filtered from the previous subset as still able to deliver this new and higher total mass to their release conditions, the cost per launch is read from the spreadsheet. For each launch system option remaining, if there are any, the fraction of mass delivery capability used per launch is multiplied by the cost per launch to find the launch cost per satellite. The launch system for which the product of this number and the number of satellites is lowest is recorded as the winning vehicle choice. If there are no options remaining, the cost is set to 1×10^{20} to indicate no launch solution for the current parameter combination.

The cost due to the satellite final mass in general, without transfer stage, was found using historical cost equations of the form $C_1 = a\,(mass^b)$, from [7]. Reduction in per-unit cost to account for the multiple satellite unit learning curve was made according to

$$C_n = C_1\ n^q \quad \text{where} \quad q = \frac{log\left[\frac{C_2}{C_1}\right]}{log(2)}. \tag{7}$$

Here $n = 1, 2, \ldots$ is the unit number of the satellite being produced and the ratio of the cost of the second unit to the cost of the first is set at about 80% [7]. This accounts,

in a general fashion, for the costs of all other subsystems besides the ACS and the optics.

III. SOLUTION METHODS

A. Brute-force Gridding Method

The discontinuous nature of cost component functions described above makes the total cost a quantity which must be minimized using non-gradient-based optimization methods. A brute-force gridding of the parameter space is the first such method used herein. Advantages of this are its simplicity and ease of implementation, and its potential for ensuring all portions of the parameter space are sampled so that regions with lowest cost are not missed. But for such lowest-cost regions in the parameter space to be sampled from, the resolution of the gridding must be small enough. Without a-priori knowledge, a fine sampling is generally needed which makes the total number of cost evaluations and computation time extremely large. This is especially true with a large number of parameters, since the number of grid points to be examined is given by the product over all parameters of the number of points into which each parameter is discretized.

B. Genetic Algorithm Methods

Genetic algorithms (GAs) work by analogy to the theory of natural evolution, with the following basic steps: An initial set of parameter combinations is randomly generated within the hypercube formed by the maximum and minimum values for each parameter. Through an encoding method, these parameter combinations are converted to corresponding strings called "chromosomes," forming an initial "population." The fitness, a strictly positive analog to the cost being minimized (usually the negative of cost plus a sufficiently large constant offset) is evaluated for each population member. A selection process is used to select a group of parents from the population in a way that favors selecting those individuals (chromosomes) with the highest corresponding fitness. The resulting parent chromosomes are paired off, and on either side of one or more splice points along their length, the string content is swapped between the parents in a pair during a "crossover" process, according to a specified crossover probability. The resulting new chromosomes are considered "children." Mutation in some form is applied to the children chromosomes. In the next iteration, or generation, the population of children chromosomes is redesignated as the population of potential parent chromosomes, the fitness of each individual is evaluated again, and so on.

Multiple GAs have results shown below, for contrast with each other as well as with the brute-force gridding method. Herein a "nominal" GA uses standard binary encoding for the chromosomes and the proportional, or "roulette wheel," parent selection method. A GA with gray code encoding and roulette selection, and one with standard binary encoding and single branch tournament selection, provide insight via comparison about the choice of encoding method and the choice of parent selection method, respectively. For all three GAs, the population size is kept constant at four times the chromosome length in bits, as recommended in [8]. A single crossover splice point (randomly placed) is used for all GAs and a crossover probability of 0.7 is used [9, 10]. The mutation probability is set using the formula

$$P_m = \frac{2 + pop}{3\ pop\ L}, \tag{8}$$

in which pop is the population size and L is the chromosome length in bits [11]. Four elite chromosomes are modeled, by directly transferring from one generation to the next the four "fittest" chromosomes without applying crossover and mutation to them, in addition to considering them as potential parents in the selection step. In all GA runs, the pseudo-random initial population is generated on the parameter hypercube using the same seed, for a fairer comparison.

IV. RESULTS

To fairly compare and contrast different solution methods, the parameters and their maximum and minimum values between which the search for the solution takes place must be kept the same when using all methods compared. Then two approaches can be used: comparing the solutions achieved while holding the amount of computation time (i.e. number of function evaluations) constant, or allowing as many function evaluations to be performed within each method as needed for it to arrive at about the same solution and comparing that computation burden. The latter approach will be taken to compare use of the nominal GA with use of the brute-force gridding method. We perform a gridding run first, then use the minimum cost found therewith as a termination threshold for a nominal GA run. The nominal GA run stops after the first generation in which one or more population members are found with corresponding cost equal to or lower than this threshold.

Due to an extremely long projected computation time for the gridding run with all twelve parameters being varied, the dimension of the problem was temporarily reduced for the gridding run, and consequently for the nominal GA run performed for comparison with it. Some heuristic judgements were made, and circular orbits and equal angular spacing were introduced to eliminate dimensions. The six parameters kept and the maximum and minimum

TABLE II

MAX. AND MIN. VALUES OF PARAMETERS USED FOR GRIDDING RUN AND NOMINAL GA RUN FOR COMPARISON WITH IT.

Parameter	Max. Value	Min. Value	# Dec. Places	# Bits
OBSAT aperture (m)	4.5	0.5	2	9
" number	5	1	0	3
" semi-major axis (m)	4.317e7	4.117e7	0	21
TRACSAT aperture (m)	4.5	0.5	2	9
" number	30	2	0	5
" semi-major axis (m)	4.327e7	2.376e7	0	25

TABLE III

SOLUTIONS FROM GRIDDING RUN AND NOMINAL GA RUN FOR COMPARISON WITH IT.

	Quantity	Gridding	Nominal GA
	# function evals	36000	288
	total cost ($B)	8.627	8.625
	actual cost ($B)	3.633	3.517
O	aperture (m)	1.5	0.6174
B	number	1	1
S	semi-major axis (m)	4.1970e7	4.2269e7
A	eccentricity	0**	0**
T	Δ long. peri. (rad)	6.282	6.282
	Δ mean anom. (rad)	0**	0**
	d_{view} (m)	2.4590e5	1.0122e5
	mean coverage (%)	0.1156	0.0239
	release mass (kg)	3042	2975
	launch vehicle	Zenit 3SL	Zenit 3SL
T	aperture (m)	2.5	2.0342
R	number	10	11
A	semi-major axis (m)	4.3270e7	3.9505e7
C	eccentricity	0**	0**
S	Δ long. peri. (rad)	0.6282	0.5712
A	Δ mean anom. (rad)	0**	0**
T	d_{detect} (m)	1.4611e7	1.1889e7
	mean coverage (%)	100	99.7287
	release mass (kg)	3204	3178
	launch vehicle	Zenit 3SL	Zenit 3SL

(**Was not a varied parameter in these reduced-dimension cases.)

values for them, are shown in Table II. For the nominal GA run to find solutions over the same space, the number of decimal places of resolution in each parameter and the corresponding allotment of bits to each parameter within the chromosomes are also listed in the fourth and fifth columns of Table II.

The number of function evaluations, total and actual costs found as a "solution," and corresponding parameter combinations are presented in Table III for the gridding run and for the nominal GA run for comparison with it. This table also includes a few key non-parameter quantities for each solution point. Fig. 1 and Fig. 2 illustrate the orbital geometry at time steps during simulations of these solution

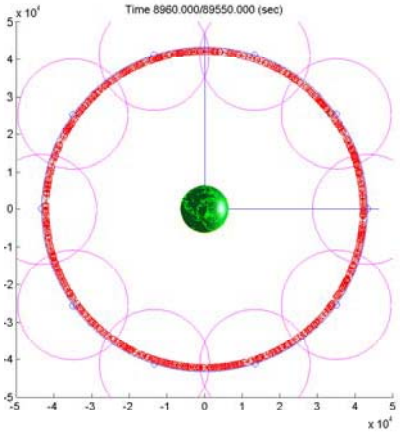

Fig. 1. Constellation found in brute-force gridding run.

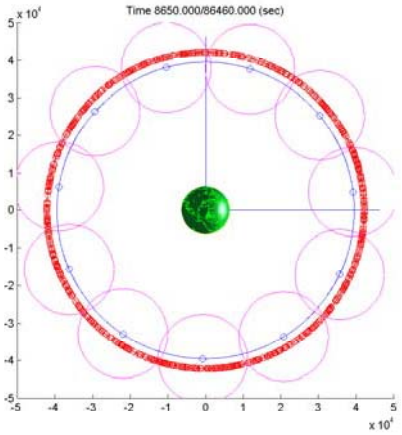

Fig. 2. Constellation found in nominal GA run for comparison.

points. The figures are to scale. The target positions are marked by small circular markers which form the thick band at the GEO radius. Also shown is the orbit of each OBSAT and a small circle, with radius equal to the viewing distance, centered at each OBSAT's current position. The TRACSAT orbits are also shown, along with much larger circles, with radius equal to the detection distance, centered at each TRACSAT's current position. These larger coverage circles overlap slightly in the figures.

Now to compare the different GAs among themselves, the other approach of fixing a constant computation time and comparing the solutions achieved is adopted. A new run using each of the three GAs was performed, this time over the full twelve-dimensional parameter space. The maximum and minimum values for all twelve parameters are shown in table IV, as are the new decimal resolutions and allotments of bits within the chromosomes. Table V shows the total and actual costs, corresponding parameters, and other quantities for the new solutions. Fig. 3 illustrates the orbital geometry at a simulation time step for the solution point found by the tournament selection GA. The same illustrations for the other two solution points are very similar to Fig. 2 and are omitted for brevity.

TABLE IV

MAXIMUM AND MINIMUM VALUES OF PARAMETERS USED FOR THE GA RUNS PERFORMED FOR COMPARISON WITH ONE ANOTHER.

Parameter	Max. Value	Min. Value	# Dec. Places	# Bits
OBSAT aperture (m)	4.5	0.5	2	9
" number	5	1	0	3
" semi-major axis (m)	4.717e7	3.717e7	0	24
" eccentricity	0.1	0	2	4
" Δ long. peri. (rad)	6.283	1.257	3	13
" Δ mean anom. (rad)	0	0	2	1
TRACSAT aperture (m)	4.5	0.5	2	9
" number	30	2	0	5
" semi-major axis (m)	4.327e7	2.376e7	0	25
" eccentricity	0.4	0	2	6
" Δ long. peri. (rad)	3.142	0.2094	3	12
" Δ mean anom. (rad)	3.142	0	3	12

TABLE V

SOLUTIONS FROM GA RUNS PERFORMED FOR COMPARISON WITH ONE ANOTHER.

Quantity		Nominal	Gray-coded	Tournament
# function evals		39360	39360	39360
total cost ($B)		8.602	8.722	9.108
actual cost ($B)		3.602	3.722	4.109
	aperture (m)	1.4628	0.6018	0.7583
O	number	1	1	2
B	semi-major axis (m)	$4.167e7$	$4.396e7$	$4.086e7$
S	eccentricity	0.0800	0.0667	0.0933
A	Δ long. peri. (rad)	2.6417	2.2643	5.1350
T	Δ mean anom. (rad)	$1e-5$	$1e-5$	0
	d_{view} (m)	$2.398e5$	$9.864e4$	$1.243e5$
	mean coverage (%)	0.0066	0.0015	0.0033
	release mass (kg)	3124	3044	3084
	launch vehicle	Zenit 3SL	Zenit 3SL	Zenit 3SL
	aperture (m)	2.0108	2.1517	2.1908
T	number	12	13	16
R	semi-major axis (m)	$4.276e7$	$4.224e7$	$3.667e7$
A	eccentricity	0.0063	0.0254	0.000
C	Δ long. peri. (rad)	1.3816	1.5055	0.6562
S	Δ mean anom. (rad)	0.8493	2.0023	2.0798
A	d_{detect} (m)	$1.175e7$	$1.258e7$	$1.280e7$
T	mean coverage (%)	100	100	100
	release mass (kg)	3114	3148	3293
	launch vehicle	Zenit 3SL	Zenit 3SL	Zenit 3SL

V. CONCLUSIONS

It is seen that the minimum cost constellation configuration for this SSA problem, with the cost component functions for performance weighted as they are, is one OBSAT travelling in a circular orbit extremely close to GEO, and just enough TRACSATs to fully cover the GEO circumference. The latter are also ideally in circular orbits with a radius very near that of GEO, and are evenly spaced in angle. The aperture size for each OBSAT is always smaller than the maximum but varies greatly among the solutions, suggesting that total cost is rather independent of this dimension. Regardless of this aperture size, an OBSAT's optics have such a short viewing distance compared to the scale of the target space that the performance cost is extremely high. For the TRACSATs, which have a larger detection distance, this is not so. For them the intuitively expected tradeoff between larger aperture size and more satellites is shown within the first pair of solutions presented, but not observed in the solutions for comparing the three varieties of genetic algorithm.

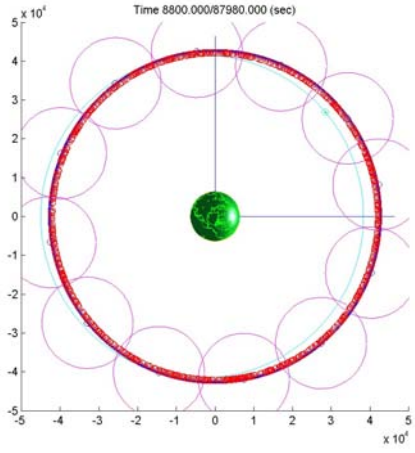

Fig. 3. Constellation found in nominal GA run.

From the actual costs of all solution designs, it seems implementation of such a hybrid constellation to achieve the stated SSA goals is not unrealistic. While expensive, it does not appear prohibitively costly within context of past satellite constellations. The very poor performance of the OBSAT in the constellation is an important reason for caution. Better modeling of the OBSAT performance with a revisit time approach, which entails a greater computational burden but is of greater interest to the users of SSA capabilities, may be needed. Demanding a circular OBSAT orbit in a retrograde direction might lead to much better results for providing useful target imaging capability.

As for evaluation of the effectiveness of the solution methods, it is seen that the GAs all perform better than a brute-force method, in terms of greatly reduced computation time, in arriving at a minimum cost solution. This conclusion is drawn even though only the nominal GA is directly compared with the gridding approach, because of the almost equivalent performance seen in Table V. As for that, no relative advantage from using gray-coding, nor from using tournament selection, is perceived for this problem.

REFERENCES

[1] U. S. Army Training and Doctrine Command, Space and Information Operations Directorate, Space Division. (2004, Sept.) Army space reference text. [Online]. Available: http://www-tradoc.army.mil/dcscd/spaceweb/internet2.htm\#CH7SEC6

[2] D. Mehrholz *et al.*, "Detection, tracking, and imaging space debris," *ESA Bulletin*, no. 109, pp. 128–134, Feb. 2002.

[3] J. Steven J. Isakowitz Joseph P. Hopkins and J. B. Hopkins, Eds., *International Reference Guide to Space Launch Systems*, 3rd ed. Reston, VA: AIAA, 1999.

[4] *Space Transportation Costs: Trends in Price Per Pound to Orbit 1990-2000*, Futron Corporation, Bethesda, MD.

[5] The Boeing Company. (2004, July) Delta IV payload planner's guide. [Online]. Available: http://www.boeing.com/defense-space/space/delta/guides.htm

[6] International Launch Services. (2004, Sept.) Atlas launch system mission planner's guide. [Online]. Available: http://www.ilslaunch.com/missionplanner

[7] D. L. Akin. (2004, Aug.) Principles of space systems design: Preliminary cost analysis. (University of Maryland course lecture slides). [Online]. Available: http://spacecraft.ssl.umd.edu/academics/483F03/

[8] E. A. Williams and W. A. Crossley, "Empirically derived population size and mutation rate guidelines for a genetic algorithm with uniform crossover," in *Soft Computing in Engineering Design and Manufacturing*, P. Chawdhry, R. Roy, and R. K. Pant, Eds. Springer-Verlag, 1998, pp. 163–172.

[9] D. E. Goldberg, *Genetic Algorithms in Search, Optimization, and Machine Learning*. Reading, MA: Addison-Wesley, 1989.

[10] J. C. Spall, *Introduction to Stochastic Search and Optimization*. Hoboken, NJ: John Wiley & Sons, Inc., 2003.

[11] T. J. Lang, "A parametric examination of satellite constellations to minimize revisit time for low earth orbits using a genetic algorithm," *Advances in Astronautical Sciences*, vol. 109, no. 1, pp. 625–640, 2002.